Available online at www.sciencedirect.com

ScienceDirect

International Journal of Pavement Research and Technology 9 (2016) 178–189

www.elsevier.com/locate/IJPRT

# Understanding effects of RAP on rheological performance and chemical composition of SBS modified binder using series of laboratory tests

Dharamveer Singh [a,*], Dheeraj Sawant [b]

[a] Dept. of Civil Engineering, Indian Institute of Technology Bombay, Mumbai 400076, India
[b] Dar Al Handasah, Hadapsar, Pune 411013, India

Received 26 March 2016; accepted 7 June 2016
Available online 14 June 2016

**Abstract**

The present study aims to evaluate rutting, fatigue, and rheological performances of a SBS co-polymer modified binder (PMB40) blended with different percentages (i.e., 0%, 15%, 25% and 40%) of reclaimed asphalt pavement (RAP) binder. The change in viscosity, mixing and compaction temperatures, and temperature susceptibility of PMB40 binder mixed with RAP were measured using Brookfield viscometer. Furthermore, linear viscoelastic range (LVE) and time-temperature sweep tests were conducted to characterize binders. The rutting and fatigue performance of PMB40 binder with varying percentages of RAP was evaluated using multi stress creep and recovery (MSCR) and linear amplitude sweep (LAS) tests, respectively. The change in chemical composition of PMB40 binder with addition of RAP was determined by Fourier transform infrared (FTIR) spectroscopy. The results showed that addition of RAP makes PMB40 binder stiff and less temperature susceptible, however, it did not change mixing and compaction temperatures significantly. Furthermore, high temperature performance grade (PG) of PMB40 binder was unaltered with addition of RAP, which is contrary to findings reported in literature. The MSCR test showed significant reduction in recovery and increment in non-recoverable creep compliance of PMB40 binder with addition of RAP, indicating a poor rutting resistance of the binder with inclusion of RAP. The LAS test showed that rate of damage increases and number of cycles to fatigue failure of PMB40 binder decreases with addition of RAP. The FTIR test confirmed increase in sulfoxide and carbonyl content with addition of RAP. A good correlation was found for ICO and ISBS indices obtained from FTIR with rheological properties of PMB40 binder. It is to be noted that the findings presented in this paper are based on one modified binder and one RAP source, thus it is recommended that effects of different RAP sources on performance of SBS modified binder be studied in detail. Further, effects of ageing (short term and long term) should be studied to have insight into characterization of RAP blended binders. It is also recommended that binder's rheological performance tests be validated by conducting laboratory tests on asphalt mixes.


*Keywords:* Reclaimed asphalt pavement; Polymer modified binder; MSCR; LAS; FTIR; Rutting

## 1. Introduction

Utilization of recycled asphalt pavement (RAP) in construction of flexible pavements can help in economic savings and conservation of natural resources. A flexible pavement experiences different weather, extreme solar radiation, temperature, and traffic loading and unloading,

* Corresponding author.
*E-mail addresses:* dvsingh@iitb.ac.in (D. Singh), dvs1292@gmail.com (D. Sawant).
Peer review under responsibility of Chinese Society of Pavement Engineering.

http://dx.doi.org/10.1016/j.ijprt.2016.06.002

which result in a stiffer and aged binder over time. Therefore, a binder extracted from RAP can have different chemical and rheological properties compared to a virgin binder [1]. The following concerns are expressed on utilization of RAP with modified and unmodified binders (i) selection of base binder (ii) change in mixing and compaction temperatures (iii) temperature susceptibility (iv) performance under different frequency, strain, and temperature (v) rutting performance (vi) fatigue performance, and (vii) chemical changes. The polymer modified binders (PMBs) are being widely used these days for construction of asphaltic layers because of their better rutting and fatigue performances [2,3]. Since performance of a PMB binder depends on strength of polymer network and its interlinking with base asphalt binder, it is important to understand change in its performance with addition of RAP [4–7]. The RAP contains stiff and aged binder, thus inclusion of RAP in a mix is expected to increase rutting performance [4–7], however, on the other hand, addition of RAP may deteriorate fatigue and low temperature cracking potential of a mix [8–11]. Thus many agencies limit use of RAP proportion for production of asphalt mixes. However, few studies are reported to evaluate effects of RAP on rheological and chemical characteristics of PMB binders. For example, Stimilli et al. [12] studied rheological and chemical changes of PMB binder with addition of a laboratory simulated RAP binder. They reported that though the addition of RAP makes the blend stiffer, the mixing temperature remains unchanged. Further, fatigue and rutting performance was not altered, and in some cases it was improved, with addition of RAP binder. Similarly, Bernier et al. [11] studied rutting performance of RAP blended binder using multiple stress creep recovery (MSCR) test and reported that rutting resistance of PMB binder decreases with addition of RAP. Hossain et al. [13] studied performance of PG76-28 with addition of RAP from two different sources using rotational viscosity and Superpave high and low temperature performance grade (PG). It was reported that high and low PG grade of the binder can change significantly with addition of RAP. Khosla et al. [4] reported that change in stiffness of binder with addition of RAP depends upon RAP source and proportions. Thus, assuming that nature of a RAP binder remains same irrespective of change in its source can lead to performance deficiencies. Similarly, Huang and Turner [7] reported that some binder may need higher PG grade adjustment than others, thus different binders and RAPs may interact differently.

Stimilli et al. [12] and Liu et al. [14] studied chemical changes of polymer binder with addition of laboratory simulated RAP using the FTIR spectroscopy. They reported that SBS content of the binder changes with inclusion of RAP, which can affect its rheological properties. Wu et al. [15] studied the change in morphology and structure of a base binder and SBS modified binder due to ageing using FTIR spectroscopy. They reported increase in carbonyl and sulfoxide group and reduction in chain segments of butadiene after ageing. Based on the literature review, it was found that majority of the reported studies considered penetration, softening point, ductility, and viscosity, and Superpave rutting and fatigue parameters to evaluate performance of PMB binder blended with RAP. The current literature have limited studies on understanding effects of RAP on rutting, and fatigue performance of polymer modified binder using recently developed advanced test such as MSCR and linear amplitude sweep (LAS) conducted with help of dynamic shear rheometer (DSR). The MSCR test measures binder's rutting performance in terms of recovery ($R$) and non-recoverable creep compliance ($J_{nr}$). The MSCR test observed to have better correlation with the rutting potential of bituminous mixes [16]. The LAS test uses viscoelastic continuum damage (VECD) theory in order to quantify the damage to asphalt binder due to repeated application of load. The major advantages of this test are that by conducting a single test, it is possible to predict the binder behaviour under varying strain levels. The LAS test has shown fair correlation with long-term pavement performance (LTPP) field fatigue cracking data [17]. Further, relationship between change in chemical properties with addition of RAP and rheological properties has not been fully explored for modified binders.

The present study considered a series of advanced tests such as MSCR to evaluate rutting performance, LAS to assess fatigue resistance of PMB40 binder blended with different percentages (i.e., 0%, 15%, 25%, and 40%) of RAP. In addition, change in mixing and compaction temperature, high PG, temperature susceptibility and linear viscoelastic range (LVE) and performance under extended frequency-temperature are reported in the present study. Further, the study evaluates change in chemical compositions of PMB40 binder with addition of RAP using FTIR technique. Moreover, correlation between FTIR indices and different rheological properties is attempted in the present study. It is expected that the outcome of the study would be helpful for agencies and industry to better characterize or utilize RAP with SBS modified binder.

## 2. Materials

In this study, a polymer modified binder (PMB 40) with 3.5% of styrene–butadiene–styrene (SBS) was selected which is commonly used for construction of flexible pavements in India. Table 1 summarizes properties of PMB40

Table 1
Characteristics of SBS polymer modified binder (PMB40).

| Physical properties | PMB 40 | Standard code |
|---|---|---|
| Penetration, @ 25 °C,100 g, 5 s | 48 | ASTM D5 [20] |
| Softening point (R & B), °C | 52 | ASTM D36 [21] |
| Ductility, @ 27 °C, cm | 132 | ASTM D113 [22] |
| Elastic recovery, @ 27 °C, % | 83 | ASTM D6084 [23] |
| Kinematic viscosity @ 135 °C, mPa·s | 1258 | ASTM D4402 [24] |
| LVE (%), 64 °C | 104 | ASTM D7175 [25] |
| High PG grade (°C) | 76 | AASHTO T 315 [26] |

binder. The high temperature PG of PMB40 was found to be PG76. The ductility and elastic recovery for PMB40 were measured to be 132 cm and 83% respectively. Penetration, softening point, kinematic viscosity at 135 °C, and LVE for PMB40 were measured to be 48 dmm, 52 °C, 1258 mPa·s, and 104%, respectively. The collected PMB40 binder satisfies the test parameters as per Indian standard. The RAP material used in this study was collected from the surface layer of six year old asphaltic pavements at Mumbai-Nashik National Highway, India. The asphalt binder originally used in the surface layer was of penetration grade 50/60. The RAP binder was unmodified binder. The extraction of binder from RAP was done in a two stage process. In first step, the aggregates were separated from RAP using centrifuge extraction method using tri-chloro ethylene (TCE) as a solvent as per ASTM D2172 [18] and then binder was extracted from solvent using rotary evaporator in accordance with ASTM 5404 [19]. The FTIR analysis was conducted on RAP extracted binder and no traces of TCE solvent were found. The characterization of RAP binder is discussed in Section 2.1.

### 2.1. Characterization of RAP binder

The extracted RAP binder was characterized by conducting various preliminary and rheological tests. The results are shown in Table 2. The softening and penetration values of extracted RAP binder were found to be 68 °C and 24 dmm, respectively. The ductility and elastic recovery value of extracted RAP binder were found to be 21.2 cm and 15%, respectively. The Brookfield viscosity of RAP binder at 135 °C was measured to be 1544 mPa·s. The LVE range of RAP binder was found to be 24%. The high temperature PG of RAP binder was measured to be 88 °C. The non-recoverable creep compliance ($J_{nr}$) and recovery ($R$) measured at 3.2 kPa and 64 °C were found to be 0.2 k $Pa^{-1}$ and 24%, respectively. The RAP binder showed 24% and 15% elastic recovery based on MSCR and ductility bath tests, respectively. A slight elastic recovery value of extracted RAP binder can be due to formation of gel like asphaltene in aged binder. The results showed that RAP binder was stiffer in nature.

### 2.2. Preparation of PMB40 and RAP blended binders

The McDaniel and Anderson [28] recommended, no grade bump upto 15% RAP, drop of one grade for RAP content between 15% and 25% and development of blending charts for RAP amount above 25%. Therefore, in the present study three different percentages: 0%, 15%, 25%, and 40% of RAP were blended with PMB40 binder. The PMB40 binder was mixed with different percentages of RAP binder using a high shear mixer at a speed of 500 rpm for 30 min at 150 °C. The blade of the mixer was moved along the depth of the container to ensure uniform mixing. The control PMB40 binder was also mixed for same duration and temperature to have a fair comparison with RAP blended binders.

## 3. Laboratory testing

The following tests: Brookfield viscosity, linear viscoelastic range, high temperature performance grade, time-temperature sweep, MSCR, LAS, and FTIR were conducted on PMB40 binder blended with 0%, 15%, 25%, and 40% of RAP. The above mentioned tests were conducted on unaged binders as the purpose of the study was to evaluate influence of RAP on rheological and chemical characteristics of PMB40 binder. However, it is recommended that a future study be conducted to check effects of ageing on properties of binder.

### 3.1. Brookfield viscosity

The viscosity of PMB40 binder containing different percentages of RAP binders (i.e., 0%, 15%, 25%, and 40%) was measured using Brookfield viscometer at 120 °C, 135 °C, 150 °C, 165 °C and 180 °C in accordance with ASTM 4402. The viscosity values of $0.17 \pm 0.02$ Pa·s and $0.28 \pm 0.03$ Pa·s are required for determining mixing and compaction temperatures, respectively. Further, viscosity and temperature relationship shown in Eq. (1) as per ASTM D2493 [29], was used to determine the temperature susceptibility of a binder. The slope VTS indicates, temperature

Table 2
Characteristics of extracted RAP binder.

| Test | Value | Standard code |
|---|---|---|
| Penetration, 25 °C (0.1 mm) | 24 | ASTM D5 [20] |
| Softening point (R & B), °C | 68 | ASTM D36 [21] |
| Ductility, 25 °C (cm) | 21.2 | ASTM D113 [22] |
| Elastic recovery, 25 °C (%) | 15 | ASTM D6084 [23] |
| Viscosity @ 135 °C (mPa·s) | 1544 | ASTM D4402 [24] |
| LVE (%), 64 °C | 24 | ASTM D7175 [25] |
| High PG grade (°C) | 88 | AASHTO T 315 [26] |
| MSCR at 64 °C, (at 3.2 kPa) | $R = 24\%$ and $J_{nr} = 0.2$ k $Pa^{-1}$ | ASTM D7405 [27] |

susceptibility coefficient. A high value of VTS indicates more temperature susceptibility of a binder and vice versa.

$$\text{LogLog}\ \eta = A + \text{VTS}\ \text{Log}(T) \quad (1)$$

where $\eta$ = viscosity in cP, $T$ = temperature in Rankine, $A$ = constant, and VTS = viscosity temperature susceptibility index.

### 3.2. Linear viscoelastic range (LVE)

Usually rheological performance tests on binders are conducted keeping strain within LVE, so inter relation between stress and strain is not affected by magnitude of stress [30]. A strain sweep test is conducted and change in complex modulus ($G^*$) corresponding to different strain levels is measured. Strain level at which $G^*$ value reduces to 95% of the initial value is reported as LVE range. In the present study, the LVE range of PMB40 binder with 0%, 15%, 25%, and 40% of RAP binder was determined using DSR at 64 °C using 25 mm diameter sample with 1 mm thickness, at a frequency of 10 rad/s in accordance with ASTM D7175 [25]. Shear strain was applied from 1% upto a certain strain limit so a reduction of 5% in $G^*$ value could be captured to estimate LVE.

### 3.3. High temperature performance grade

A temperature at which minimum value of Superpave rutting parameter, $G^*/\sin\delta$ satisfies termed as high temperature PG of a binder. The limiting $G^*/\sin\delta$ value for unaged binder is 1 kPa. In the present study, $G^*$ and $\delta$ values of PMB40 binder with different percentages of RAP (0%, 15%, 25%, and 40%) were measured at various temperatures (i.e., 58 °C, 64 °C, 70 °C, 76 °C, 82 °C, and 88 °C) with an interval of 6 °C. The test was conducted using 25 mm diameter sample with 1 mm thickness in DSR keeping strain level within LVE subjected to 10 rad/s as per AASHTO T 315 [26].

### 3.4. Time-temperature sweep test

Asphalt binder is a viscoelastic material, thus its behaviour is time and temperature dependent. Time temperature superposition principle is used to plot master curve to predict the shear modulus of a binder over an extended range of frequency, The time temperature sweep test was conducted on PMB40 binder blended with 0%, 15%, 25%, and 40% of RAP binder at 50 °C, 60 °C, 70 °C, 80 °C, 90 °C with frequency from 1 rad/s to 100 rad/s. The test was conducted using 25 mm diameter sample with 1 mm thickness and at a strain of 4%. The master curves for complex modulus ($G^*$), storage modulus ($G'$), and loss modulus ($G''$) were plotted at 70 °C reference temperature. The shift factor, a($T$) was determined by the William Lendel Ferry (WLF) Eq. (2) [31] shown below. The reduced frequency can be obtained using Eq. (3) and thereafter, master curves can be modelled using Christensen, Anderson and Marasteanu (CAM) model [32–33] as shown in Eq. (4).

$$\log a(T) = \frac{-C_1(T - T_r)}{C_2 + T - T_r} \quad (2)$$

where

$C_1$ and $C_2$ are constants, $T$ = testing temperature, and $T_r$ = reference temperature.

$$\omega_r = \omega * 10^{\log a(T)} \quad (3)$$

where

$\omega_r$ = reduced frequency in rad/s, and $\omega$ = testing frequency in rad/s.

$$G^*(\omega) = G_g\left[1 + \left\{\frac{\omega_r}{\omega_c}\right\}^{(log2/R)}\right]^{-R/log2}. \quad (4)$$

where

$G^*(\omega)$ = predicted $G^*$ value, $G_g$ = Glassy modulus, assumed equal to 1 GPa, $\omega_c$ = crossover frequency in rad/s, $R$ = rheological index ($v = \log 2/R$), and $C_1$, $C_2$ are constant. The Eq. (4) can be solved using Excel Solver.

### 3.5. Multiple stress creep recovery (MSCR) test

The MSCR test measures binder's rutting performance in terms of recovery ($R$) and non-recoverable creep compliance ($J_{nr}$). The test involves 10 loading and unloading cycles with a creep load for 1 s followed by a recovery period of 9 s under 0.1 kPa and 3.2 kPa stress levels. Fig. 1 shows loading and unloading cycles in MSCR test. In the present study, the MSCR test was conducted on PMB40 binder with 0%, 15%, 25%, and 40% of RAP binder at 64 °C using 25 mm diameter sample with 1 mm thickness, at 10 rad/s as per ASTM D7405 [27]. The $R$ indicates elastic recovery of a binder after removal of the applied stress (unloading stage). A binder with high value of recovery may produce less permanent deformation in a pavement. Percent recovery ($e_r$, %) for each cycle at creep ($\tau$, Pa) is given by Eq. (5), and average percent recovery ($R_\tau$,%) at creep ($\tau$, Pa) for 10 cycles is given by Eq. (6). A high $J_{nr}$ value indicates that a binder is more rutting susceptible

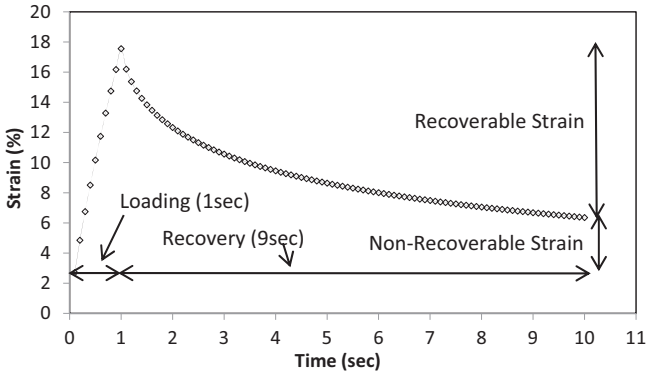


Fig. 1. Loading and unloading cycle in MSCR test.

and vice versa. The ($J_{nr}$, k Pa$^{-1}$) for each cycle at creep stress ($\tau$, kPa) can be estimated from Eqs. (7) and (8).

$$e_r(\tau) = \frac{(e_1 - e_{10}) * 100}{e_1} \quad (5)$$

where $e_1$ = strain at the end of 1 s, $e_{10}$ = strain at the end of 10 s

$$ER_\tau = \frac{SUM(e_r(\tau))}{10} \quad (6)$$

$$J_{nr}(\tau) = \frac{e_{10}}{\tau} \quad (7)$$

Non-recoverable creep compliance ($J_{nr}$, k Pa$^{-1}$) at creep ($\tau$, kPa) for 10 cycles is given by,

$$J_{nr}(\tau) = \frac{SUM(J_{nr}(\tau))}{10} \quad (8)$$

### 3.6. Linear amplitude sweep (LAS) test

The LAS test is conducted to study the resistance of a binder to fatigue failure. This test is performed in two stages (i) first frequency sweep (0.2–30 Hz) at constant amplitude strain within linear visco-elastic range level (0.1%) is carried out in order to get information regarding undamaged material property ($\alpha$), and then (ii) amplitude sweep test (0–30%) at frequency level of 10 Hz is conducted. During amplitude sweep test, loading amplitude was linearly increased from 0% to 30%. The damage to the binder at any time can be expressed as shown in Eq. (9) [34–35].

$$D(t) \cong \sum_{i=1}^{N} [\pi \gamma_0^2 (C_{i-1} - C_i)]^{\alpha/1+\alpha} (t_i - t_{i-1})^{1/1+\alpha} \quad (9)$$

where $C_t = G^*(t)/G^*(\text{initial})$ = integrity parameter; $\gamma_0$ = applied strain level (%); $G^*$ = complex modulus (MPa); $\alpha = 1/m$ where $m$ is the slope of logarithmic plot between storage modulus and applied frequency; $t$ = testing time (second). During the testing phase, both $C_t$ and $D_t$ are recorded. Power law model is used in order to develop relationship between damage to the integrity parameter as given by Eq. (10).

$$C(t) = C_0 - C_1 D^{C_2} \quad (10)$$

where $C_1$ and $C_2$ are curve fitting equations. The damage value at failure corresponds to maximum peak shear stress is further calculated as given in Eq. (11).

$$D_f = \left( \frac{C_0 - C_{\text{at peak stress}}}{C_1} \right)^{1/C_2} \quad (11)$$

Finally, fatigue equation can be expressed as given by Eq. (12);

$$N_f = A(\gamma_{max})^{-B} \quad (12)$$

where $A = \frac{f \times D_f \times (1+(1-C_2)\alpha)}{(1+(1-C_2)\alpha) \times (\pi C_1 C_2)^{\alpha}}$, $f$ = loading frequency in Hz; $\gamma_{max}$ = maximum expected binder strain in pavement and $B = 2\alpha$.

The test was conducted on PMB40 binder containing different percentages of RAP (0%, 15%, 25%, and 40%) using DSR at 25 °C on sample of having 8 mm diameter and 2 mm gap between parallel plates as per AASHTO TP101 [34].

### 3.7. FTIR test

The FTIR was used to identify presence of different functional groups in the binder. The FTIR test on PMB40 binder with different proportion of RAP (0%, 15%, 25%, and 40%) was carried out on a solution (trichloro ethylene) having a concentration of 75 g/l in accordance with a procedure outlined in Belgian Road Research Centre report ME 83/13 [36]. The test was conducted using Bruker 3000 Hyperion Microscope with Vertex 80 FTIR system. Table 3 summarizes FTIR indices for different functional groups. The effects of RAP on PMB40 binder were analysed by estimating three indices: ISO, ICO and ISBS, suggested by Liu et. al. [14] using Eqs. (13)–(15), respectively. In the above indices, ICO indicates ageing due to ketones (C= O) at 1700 cm$^{-1}$ peak, ISO indicates ageing due to sulfoxide (S=O) at 1030 cm$^{-1}$ peak, and ISBS indicates the presence of SBS polymer around 966 cm$^{-1}$ and 699 cm$^{-1}$ peak. The denominator indicates aliphatic structure.

$$\text{ICO} = \frac{\text{Area around } 1700 \text{ cm}^{-1}}{\text{Area around } 1460 \text{ cm}^{-1} \text{ and Area around } 1375 \text{ cm}^{-1}} \quad (13)$$

$$\text{ISO} = \frac{\text{Area around } 1030 \text{ cm}^{-1}}{\text{Area around } 1460 \text{ cm}^{-1} \text{ and Area around } 1375 \text{ cm}^{-1}} \quad (14)$$

$$\text{ISBS} = \frac{\text{Area around } 966 \text{ cm}^{-1} + \text{Area around } 699 \text{cm}^{-1}}{\text{Area around } 1460 \text{ cm}^{-1} \text{ and Area around } 1375 \text{ cm}^{-1}} \quad (15)$$

## 4. Results and discussion

### 4.1. Brookfield viscosity

Fig. 2 shows Brookfield viscosity of PMB40 binder blended with different percentages of RAP (0%, 15%,

Table 3
FTIR indices for different chemical compositions.

| Peak (cm$^{-1}$) | Lower limit (cm$^{-1}$) | Upper limit (cm$^{-1}$) |
|---|---|---|
| 1700 (Carbonyl) | 1660 | 1753 |
| 1030 (Sulfoxide) | 994 | 1047 |
| 966 (SBS polymer) | 956 | 980 |
| 699 (SBS polymer) | 692 | 712 |
| 1460 (Aliphatic structures) | 1400 | 1525 |
| 1375 (Aliphatic structures) | 1350 | 1390 |

25%, and 40%) at varying temperatures i.e. 120 °C, 135 °C, 150 °C, 165 °C and 180 °C. It can been seen that viscosity of PMB40 binder is unaltered at high temperatures ⩾135 °C with addition of RAP binder. However, at 120 °C, addition of 25% and 40% RAP showed high viscosity compared to virgin PMB40, indicating stiffer nature of binder with inclusion of RAP. A similar trend of viscosity with addition of RAP was observed by Hossain et al. [13] for modified binders.

### 4.2. Temperature susceptibility

The temperature susceptibility of PMB40 with addition of RAP was evaluated using A-VTS relationship (Eq. (1)). Table 4 summarizes A and VTS values of the PMB40 binder with varying percentages of RAP. The slope VTS indicates, temperature susceptibility coefficient. It can be seen that VTS value of PMB40 binder decreases with addition of RAP, showing that inclusion of RAP can help improve temperature susceptibility of PMB40 binder, which is consistent with the results reported by Kim et al. [37]. It can be due to stiffening effect of RAP. Similarly, a value decreases with an increase in RAP amount.

### 4.3. Mixing and compaction temperatures

Table 5 summarizes results of mixing and compaction temperatures. The average mixing temperature of PMB40 binder mixed with 0%, 15%, 25%, and 40% RAP was measured to be 183.5 °C, 185 °C, 186.5 °C, and 190 °C, respectively. The maximum mixing temperature was found to be for 40% RAP binder, which is approximately 7 °C more compared to control PMB40 binder, otherwise the mixing temperature does not show appreciable change with addition of RAP, and it falls within the stipulated range of temperature for modified binders as per Indian standard. Similarly, average compaction temperature of PMB40 binder mixed with 0%, 15%, 25%, and 40% RAP was measured to be 169 °C, 171 °C, 172 °C, and 174.5 °C, respectively. The maximum compaction temperature was observed to be for PMB40 with 40% RAP, which is approximately 6 °C more than that of control PMB40 binder. No significant difference was visible for 15% and 25% RAP. Overall, not much change was noticed in mixing and compaction temperatures of PMB40 with addition of RAP binder. Colbert and You [38] and Stimilli et al. [12] found similar results for mixing and compaction temperature with addition of RAP. The results indicate that addition of RAP makes PMB40 binder stiffer, less temperature susceptible, and unaltered mixing and compaction temperature.

Table 4
A–VTS value of PMB40 binder with varying RAP amounts.

| RAP (%) | A | VTS |
|---|---|---|
| 0 | 8.9358 | −2.9467 |
| 15 | 8.7796 | −2.8912 |
| 25 | 8.6811 | −2.8561 |
| 40 | 8.2367 | −2.7006 |

Table 5
Mixing and compaction temperatures for PMB 40 blended with RAP.

| RAP (%) | Mixing temp. (°C) | | Compaction temp. (°C) | |
|---|---|---|---|---|
| | Lower limit | Upper Limit | Lower limit | Upper limit |
| 0 | 180 | 187 | 166 | 172 |
| 15 | 181 | 189 | 168 | 174 |
| 25 | 183 | 190 | 169 | 175 |
| 40 | 186 | 194 | 172 | 177 |

### 4.4. Linear viscoelastic range

The LVE of PMB40 binder with different percentages of RAP binder measured at 64 °C is shown in Fig. 3. It can be seen that addition of RAP binder causes a reduction in the LVE range of PMB40 binder, thus stiffer nature of binder. The LVE range of PMB40 with 0%, 15%, 25%, and 40% of RAP was found to be 104%, 100%, 87%, and 79%, respectively. The LVE range reduces from 104% for virgin PMB40 to 79% for 40% of RAP content. This change may be a combined effect of stiffening of binder due to addition of RAP and damage to polymer network. The change in the polymer content was verified by means of FTIR testing performed on the sample.

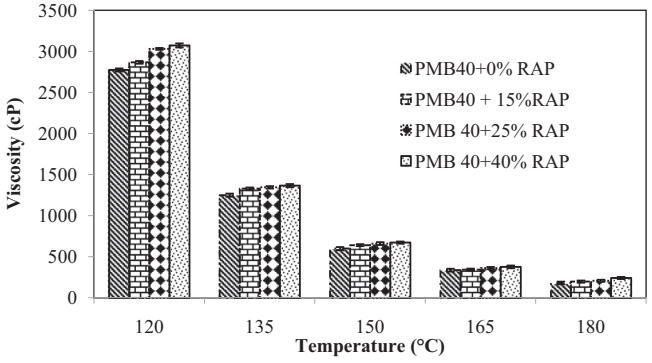


Fig. 2. Brookfield viscosity of PMB 40 with varying percentages of RAP.

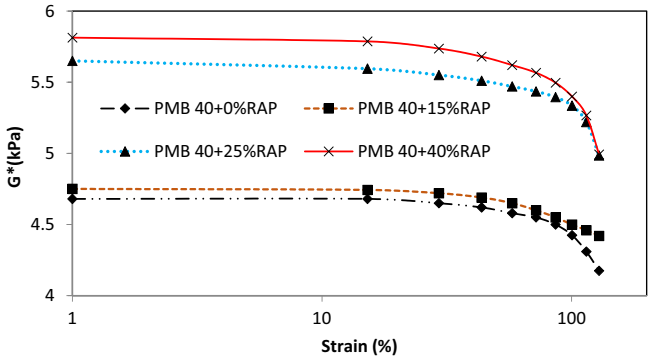


Fig. 3. LVE range of PMB 40 binder with varying percentages of RAP.

### 4.5. High temperature performance grade

Fig. 4 shows the plot of Superpave rutting parameter ($G^*/\sin\delta$) versus temperature for PMB40 mixed with different percentages of RAP. The PMB40 binder with 15% RAP showed a similar trend of $G^*/\sin\delta$, like a control PMB40 binder. However, addition of higher amounts of RAP (i.e., 25% and 40% RAP) resulted in increased values of $G^*/\sin\delta$. Thus, it can be concluded that PMB40 binder becomes stiffer (high rut resistant) with addition of higher percentages of RAP. The continuous high PG of PMB40 binder with 0%, 15%, 25%, and 40% was found to be 81 °C, 82 °C, 82 °C and 83 °C, respectively, indicating no significant change in high PG with addition RAP. This finding is contrary to what is being recommended by McDaniel and Anderson [28] that addition of 25% RAP increases one PG grade, and 40% RAP expected to increase more. Similar findings are reported by Khosla et al. [4] and Huang and Turner [7]. It can be concluded that effects of RAP largely depend on quality of RAP, thus it's important that a proper characterization should be undertaken at material testing phase.

### 4.6. Time temperature superposition

Fig. 5(a)–(c) shows master curve for $G^*$, $G'$, and $G''$, respectively, developed at a reference temperature of 70 °C for PMB40 binder blended with different percentages of RAP. The $G'$ indicates amount of energy stored in binder, hence a higher G′ would indicate better recovery and elastic response. Similarly, $G''$ represents amount of energy lost and hence an increase in $G''$ is an indication of reduction in elastic response of a binder.

Fig. 5(a) shows that addition of RAP resulted in stiffer binder throughout the range of frequency or temperature, except at high temperature (at low reduced frequency) where all binders showed similar performance. Both 25% and 40% RAP showed similar trend on stiffness of binder. The results were in line with the findings of Bernier et al. [11] and Rahimzadeh [39]. Fig. 5(b) shows that at higher temperatures (low reduced frequency), control PMB40 showed higher $G'$, thus a better performance. The PMB40 with 40% RAP had lower storage modulus, which

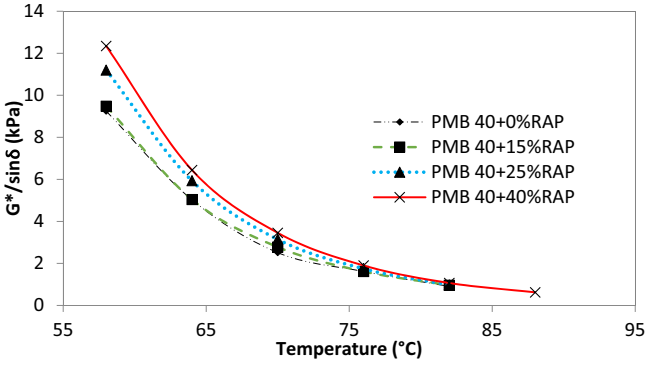


Fig. 4. Rutting parameter for PMB40 for varying percentages of RAP.

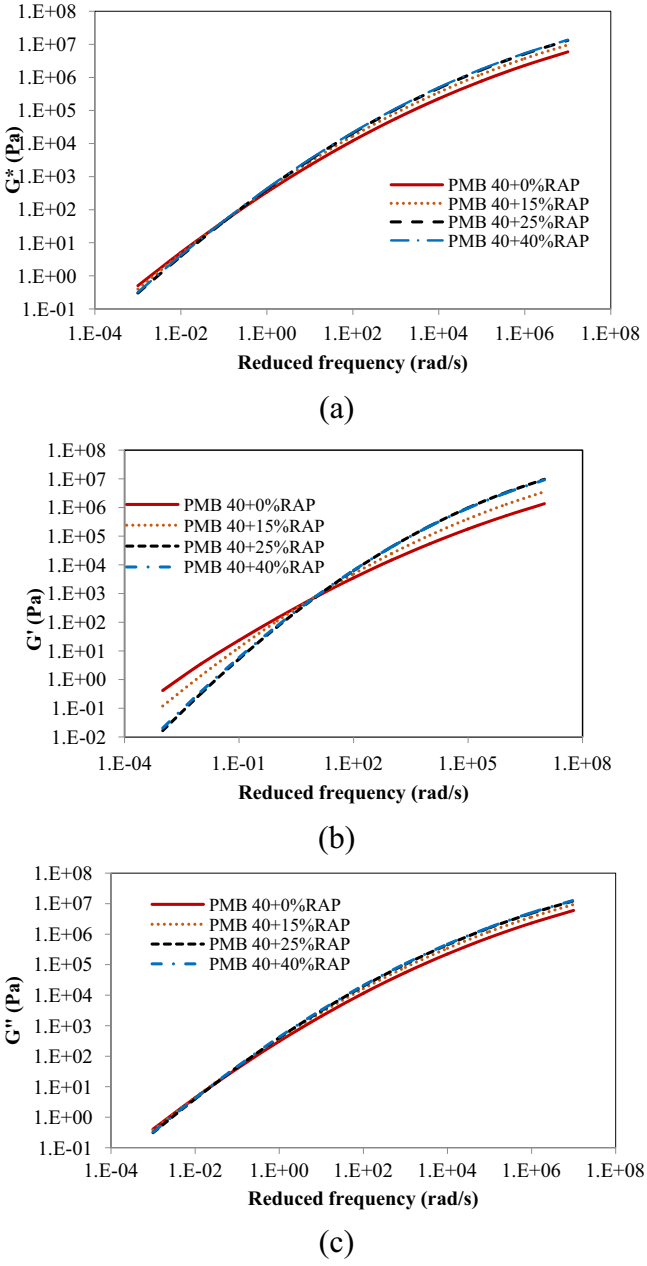


Fig. 5. Master curve for PMB40 for varying percentages of RAP (a) complex modulus – $G^*$, (b) storage modulus – $G'$, and (c) loss modulus – $G''$.

showed diminishing effects of polymer network at higher temperatures. At lower temperatures (higher reduced frequencies), the higher RAP content had higher storage modulus, which is expected due to stiffening effect and glassy state of the binder. Fig. 5(c) showed that addition of RAP resulted in higher magnitude of $G''$, throughout frequency range, and found to be maximum for 40% RAP.

### 4.7. Rutting performance from MSCR test

Fig. 6(a) shows measured strain for PMB40 binder with different percentages of RAP, subjected to 3200 Pa

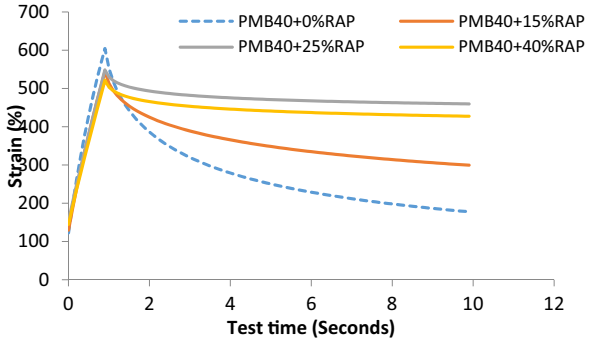


(a)

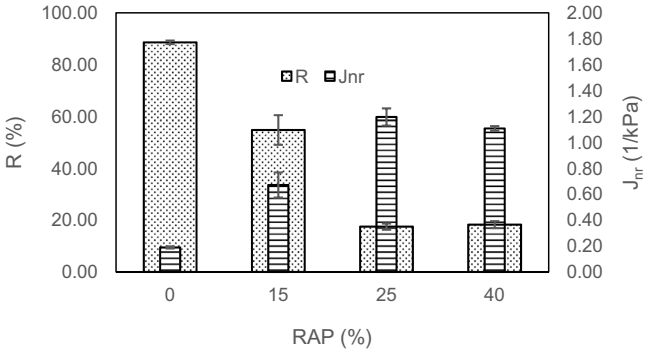


(b)

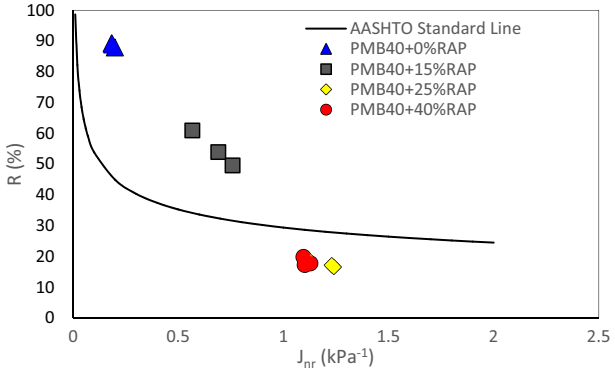


(c)

Fig. 6. MSCR test results for PMB40 for varying percentages of RAP (a) strain curve, (b) change in recovery and $J_{nr}$, and (c) relationship between $R$ and $J_{nr}$.

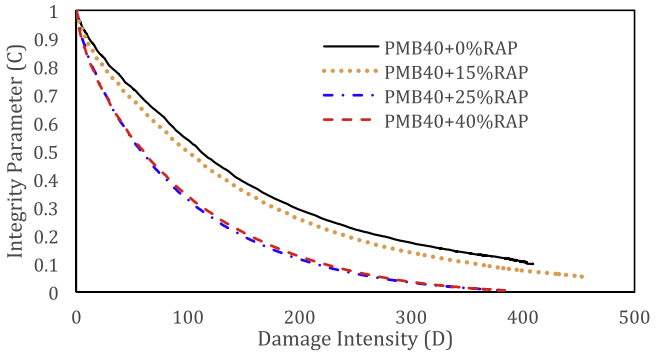


(a)

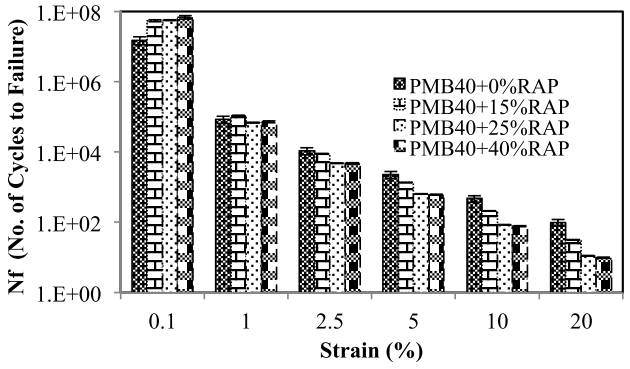


(b)

Fig. 7. LAS test results for PMB40 with varying percentages of RAP (a) damage intensity versus integrity parameter, (b) variation of fatigue cycles with strain.

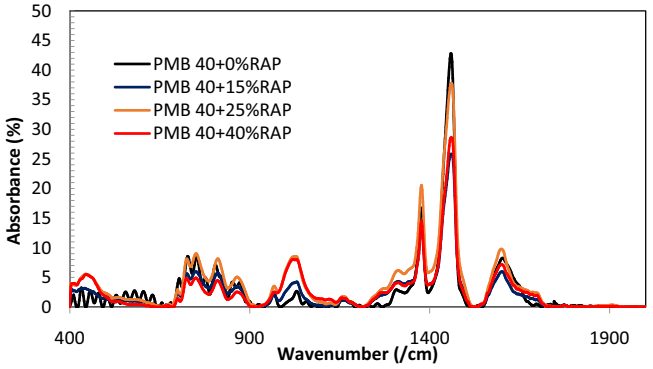


Fig. 8. FTIR plot for PMB40 with varying percentages of RAP.

at 64 °C. It can be seen that PMB40 with RAP shows lower strain, indicating stiffer nature of the binder. However, permanent strain value increases with an increase in RAP. It can be observed that addition of RAP binder resulted in significant reduction in $R$ (Fig. 6(b)). For example, R value for PMB40 with 0%, 15%, 25% and 40% of RAP was found to be 89%, 55%, 17%, and 18%, respectively. The maximum reduction was noted with RAP content of 25% and higher. Similarly, $J_{nr}$ value of PMB40 binder increases with an increase in RAP (Fig. 6(b)). For instance, $J_{nr}$ increased from 0.2 k $Pa^{-1}$ to 0.7 k $Pa^{-1}$, 1.2 k $Pa^{-1}$, 1.1 k $Pa^{-1}$ with an increase in RAP content from 0% to 15%, 25% and 40%, respectively. The reduced $R$ and increased $J_{nr}$ showed significantly poor rutting resistant of PMB40 binder with RAP binder. Thus agencies should be cautious for adding RAP with SBS modified binder. It is noted that Superpave rutting parameter ($G^*/\sin\delta$) also indicated stiff nature of binder with addition of RAP, however, this test cannot show recovery potential and true behaviour of binder sample under loading and unloading. Therefore, MSCR test is

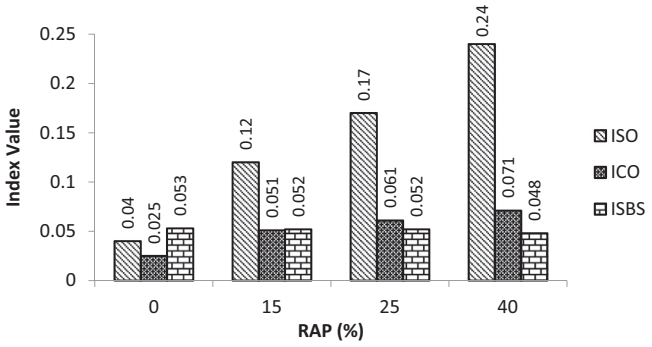


Fig. 9. FTIR indices for PMB40 blends.

preferred to evaluate rutting potential of a binder. The plot between $J_{nr}$ and $R$ (Fig. 6(c)) showed that points for PMB40 with RAP binder falls below the AASHTO standard line. A point above AASHTO standard line shows presence of polymer, while a point below the standard line indicates reduced or diminishing effects of polymer. It can be concluded that addition of RAP binder might have resulted in damage of polymer network of PMB40 binder, and hence poor rutting performance. The change in RAP content from 25% to 40% did not show much variation in $J_{nr}$ and $R$.

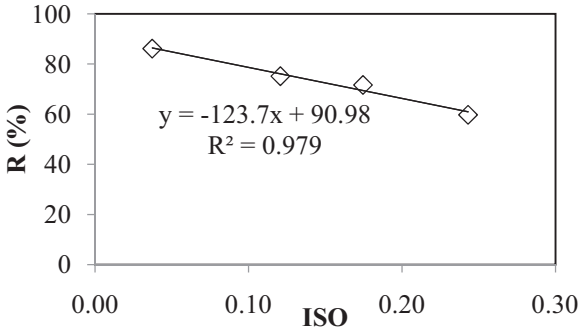


(a)

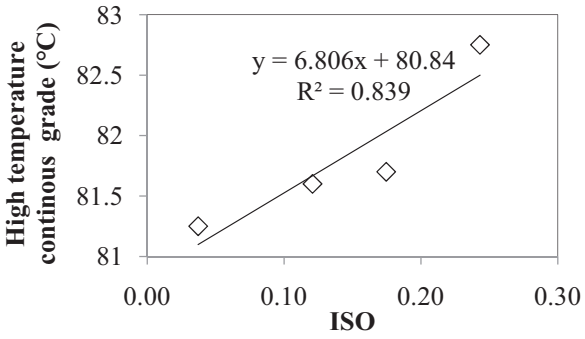


(b)

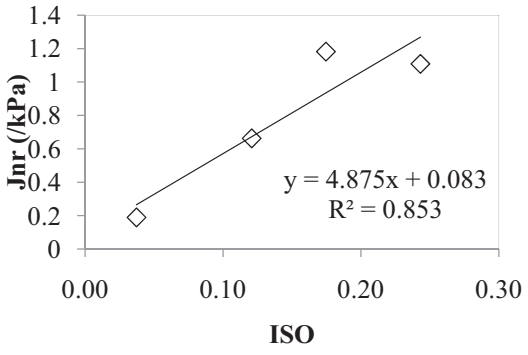


(c)

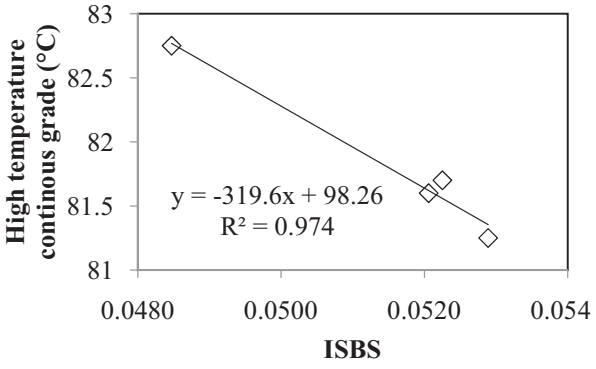


(d)

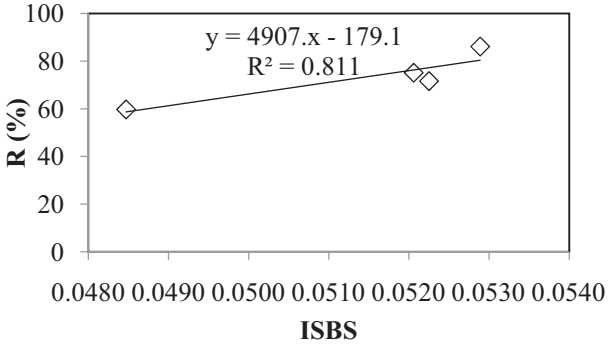


(e)

Fig. 10. Plot between FTIR indices and PMB40 properties (a) ISO versus $J_{nr}$ (b) ISO versus high temperature (c) ISO versus $R$ (d) ISBS versus high temperature (e) ISBS versus $R$.

### 4.8. Fatigue performance from LAS test

Fig. 7(a) shows a relationship between damage intensity ($D$) and integrity parameter ($C$) for PMB40 with varying amounts of RAP. Value of $C$ equals to 1 represents the highest integrity with no damage, whereas $C$ equal to zero represents complete failure to a material. Fig. 7(a) shows that the rate of decrease of $C$ increases with addition of RAP, indicating rapid damage to performance of PMB40 binder with RAP binder. It can also be observed that at any particular level of $D$, $C$ is highest for control PMB40 binder followed by 15% RAP, 25% and 40% RAP binders.

The LAS test gives results in terms of number of load repetitions of ESAL ($N_f$) to failure versus applied shear strain. The $N_f$ obtained from the calculation was normalised to 1 million ESALs. Fig. 7(b) shows the results of LAS test conducted on PMB40 binder with different percentages of RAP. From the results it can be seen that at lower strain value (0.1%), fatigue resistance of PMB40 binder increased with inclusion of RAP, though it did not change much with addition of higher percentages of RAP. At such low strain, binder exhibits undamaged property and effects of RAP may not be visible. However, with increase in strain, the trend completely reverses, and higher RAP contents showed least fatigue resistance. The addition of RAP causes stiffer nature of PMB40 binder thus reduced fatigue life. This behaviour can be attributed to the addition of the stiffer RAP binder as well as replacement of the polymer or damage to polymer network with RAP binder which causes reduction in its fatigue resistance at higher strain.

### 4.9. Chemical composition using FTIR

Fig. 8 shows the FTIR spectrum of PMB40 binder with different percentages of RAP. The sulfoxide content (around 1030/cm) and carbonyl content (around 1700/cm), and SBS polymer content (around 966/cm and 699/cm) were considered to understand change in chemical composition of PMB40 binder with addition of RAP. Fig. 9 shows ISO, ICO, and ISBS indices for PMB40 binder blended with varying percentages of RAP. It can be seen that addition of RAP increases ISO and ICO indices, indicting oxidized nature of PMB40 with RAP binder. The PMB40 blends showed the presence of polymer with peak at the SBS region. The ISBS index did not show much reduction with addition of RAP except at 40% RAP. The results show that ageing behaviour of RAP binder is dominant which may have resulted in breaking of polymer chains/interlinking [12,15].

### 4.10. Correlation between FTIR indices and rheological properties

The correlation between FTIR indices (ISO, ICO, ISBS) and $J_{nr}$, high temperature continuous PG, and $R$ are shown in Fig. 10. A good correlation was observed between ISO and $R$ (%) ($R^2 = 0.98$), ISO and high temperature continuous PG ($R^2 = 0.84$), and ISO and $J_{nr}$ ($R^2 = 0.85$). It can be seen that with an increase in ISO, $J_{nr}$ and high temperature continuous PG of binder increase, and R decreases, indicating a trend of aged and stiffer binder. The polymer index i.e. ISBS gave a good correlation with high temperature continuous PG ($R^2 = 0.97$) and $R$ ($R^2 = 0.81$). It can be seen that high temperature continuous PG decreases and ER increases with an increase in ISBS value, showing importance of polymer presence (Fig. 10).

## 5. Conclusions

The present study characterizes performance of SBS polymer modified binder blended with different percentages (i.e., 0%, 15%, 25% and 40%) of RAP using series of advanced tests such as MSCR, LAS, and FTIR. The following conclusions can be drawn based on the results and discussion presented above.

(a) The PMB40 binder becomes stiffer with addition of RAP, however, its viscosity did not change significantly at high temperature. Thus mixing and compaction temperature of PMB40 binder did not change to a great extent with addition of RAP. Addition of RAP improved temperature susceptibility of PMB40 binder.
(b) LVE range of PMB40 binder reduced drastically with addition of RAP, indicating adverse effects of aged binders on modified binder.
(c) The high temperature continuous PG of PMB40 did not change much with addition of RAP, which is contrary to the findings reported in literature. No grade change was found with addition of 25% RAP and 40% RAP.
(d) The MSCR test showed that addition of RAP can cause significant reduction in $R$ and increment in $J_{nr}$ of PMB40 binder, thus indicating poor rutting performance of PMB40 binder with RAP.
(e) The LAS showed that damage rate of PMB40 binder increases rapidly with addition of RAP. The number of cycles to fatigue failure decreases with an increase in RAP amount.
(f) The FTIR for PMB40 showed increased ISO and ICO, and reduced ISBS with addition of RAP, indicating stiffening effect and reduced polymer contribution. A good correlation was observed between ISO and $R$, $J_{nr}$, and continuous high temperature PG.

## 6. Limitation and recommendations

The study uses one source of RAP, and it is recommended that effects of RAP sources on performance of SBS modified binder be studied in details. Further, the present study conducted tests on unaged binder, with aim to see a trend in performance parameters, however, it is

important that effects of ageing (short term and long term) be studied in detail for better characterization of RAP blended binder. Further, it is recommend that binder rheological performance tests be validated by conducting laboratory tests on asphalt mixes. Also, the current study used a RAP which was collected from a flexible pavement of 6 years of age, thus effects of older RAP (say 10–15 years of aged) on performance of binders should be studied in future. The validity of LAS test to predict fatigue performance of binder should be verified in lab by conducting tests on mixes. In addition, double edge notch test (DENT) which is based on fracture mechanics concept may be tried to evaluate ductile failure resistance of binders.

## Acknowledgements

The authors would like to acknowledge the funding support of Council of Scientific and Industrial Research (CSIR), India for this project no. 14CSIR002. Also, thanks to Mr. Mohammed Azharuddin, Junior Technical Superintendent at Advanced Pavement Laboratory for providing laboratory technical support for the project.

## References

[1] I.L. Al-Qadi, M. Elseifi, S.H. Carpenter, FHWA-ICT-07-001: Reclaimed Asphalt Pavement – A Literature Review, Illinois Center for Transportation, 2007.
[2] Y. Yildirim, Polymer-modified asphalt binders, Constr. Build. Mater. 21 (2007) 66–72.
[3] H.L. Von Quintus, J. Mallela, M.S. Buncher, Quantification of effect of polymer-modified asphalt on flexible pavement performance, Transp. Res. Rec.: J. Transp. Res. Board, No. 2001, Transportation Research Board of the National Academies, Washington, D.C., 2007, pp. 141–154.
[4] N.P. Khosla, Nair, Harikrishnan, Beth Visintine, Glen Malpass, Effect of reclaimed asphalt and virgin binder on rheological properties of binder blends, Int. J. Pavement Res. Technol. 5 (2012) 317–325.
[5] A. Hussain, Q. Yanjun, Effect of reclaimed asphalt pavement on the properties of asphalt binder, Sci. Direct Procedia Eng. 54 (2013) 840–850.
[6] Z. Hossain, M. Zaman, P. Solanki, S. Ghabchi, D.V. Singh, A. David, S. Lewis, Implementation of MEPDG for Asphalt Pavement with RAP Final Report, University of Oklahoma, Oklahoma Transportation Center, 2013.
[7] S. Huang, T.F. Turner, Aging characteristics of RAP blend binders: rheological properties, Am. Soc. Civil Eng. 26 (2014) 966–973.
[8] T.W. Kennedy, W.O. Tam, M. Solaimanian, Effect of Reclaimed Asphalt Pavement on Binder Properties Using the Superpave System Publication Research Report 1205-1, Center for Transportation Research, Bureau of Engineering Research, University of Texas at Austin, 1998.
[9] K.W. Lee, N. Soupharath, N. Shukla, C.A. Franco, F.J. Manning, Rheological and mechanical properties of blended asphalt containing recycled asphalt pavement binders, J. Assoc. Asphalt Paving Technol. 68 (1999) 89–125.
[10] B.Z. Huang, G. Li, D. Vukosavljevic, X. Shu, B. Edgan, Laboratory investigation of mixing HMA with RAP, J. Transp. Res. Board, 2005, pp. 37–45, Transportation research record no. 1929 Washington, D.C..
[11] A. Bernier, A. Zofka, I. Yut, Laboratory evaluation of rutting susceptibility of polymer-modified asphalt mixtures containing recycled pavements, Constr. Build. Mater. (31) (2012) 56–58
[12] A. Stimilli, G. Ferrotti, C. Conti, G. Tosi, F. Canestrari, Chemical and rheological analysis of modified bitumens blended with artificial reclaimed bitumen, Constr. Build. Mater. (63) (2014) 1–10
[13] Z. Hossain, P. Solanki, M. Zaman, Mechanistic evaluation of recovered materials from recycled asphalt pavement, in: Geo Congress 2012, Oakland, CA, 2012.
[14] G. Liu, E. Nielsen, J. Komacka, G. Leegwater, M. Ven, Influence of the soft bitumen on the chemical and rheological properties of reclaimed polymer-modified binders from the "old" surface-layer asphalt, Constr. Build. Mater. (79) (2015) 129–135
[15] S.P. Wu, L. Pang, L.T. Mo, Y.C. Chen, G.J. Zhu, Influence of aging on the evolution of structure, morphology and rheology of base and SBS modified bitumen, Constr. Build. Mater. (23) (2009) 1005–1010
[16] J. D'Angelo, R. Kluttz, R.N. Dongre, K. Stephens, L. Zanzotto, Revision of the superpave high temperature binder specification: the multiple stress creep recovery test (with discussion), J. Assoc. Asphalt Paving Technol. 76 (2007) 123–162.
[17] C. Hintz, R. Velasquez, C. Johnson, H. Bahia, Modification and validation of linear amplitude sweep test for binder fatigue specification, Transp. Res. Rec.: J. Transp. Res. Board 2207 (2011) 99–106.
[18] ASTM International, ASTM D2172/D2172M-11: Standard Test Methods for Quantitative Extraction of Bitumen from Bituminous Paving Mixtures, American Society for Testing and Materials, Pennsylvania, USA, 2011.
[19] ASTM International, ASTM D5404/D5404M-12: Standard Practice for Recovery of Asphalt from Solution Using the Rotary Evaporator, American Society for Testing and Materials, Pennsylvania, USA, 2012.
[20] ASTM International, ASTM D5/D5M-13: Standard Test Method for Penetration of Bituminous Materials, American Society for Testing and Materials, Pennsylvania, USA, 2013.
[21] ASTM International, ASTM D36/D36M-12: Standard Test Method for Softening Point of Bitumen (Ring and Ball Apparatus), American Society for Testing and Materials, Pennsylvania, USA, 2012.
[22] ASTM International, ASTM D113–07: Standard Test Method for Ductility of Bituminous Materials, American Society for Testing and Materials, Pennsylvania, USA, 2007.
[23] ASTM International, ASTM D6084/D6084M-07: Standard Test Method for Elastic Recovery of Asphalt Materials by Ductilometer, American Society for Testing and Materials, Pennsylvania, USA, 2007.
[24] ASTM International, ASTM D4402/D4402M-13: Standard Test Method for Viscosity Determination of Asphalt at Elevated Temperatures using a Rotational Viscometer, American Society for Testing and Materials, Pennsylvania, USA, 2013.
[25] ASTM International, ASTM D7175–08: Standard Test Method for Determining the Rheological Properties of Asphalt Binder using a Dynamic Shear Rheometer, American Society for Testing and Materials, Pennsylvania, USA, 2008.
[26] AASHTO, AASHTO T315–10: Determining the Rheological Properties of Asphalt Binder using a Dynamic Shear Rheometer, American Association of State Highway and Transportation Officials, Washington D.C., USA, 2010.
[27] ASTM International, ASTM D7405–10a: Standard Test Method for Multiple Stress Creep and Recovery (MSCR) of Asphalt Binder using a Dynamic Shear Rheometer, American Society for Testing and Materials, Pennsylvania, USA, 2010.
[28] R. McDaniel, R.M. Anderson, Recommended use of reclaimed asphalt pavement in the Superpave mix design method: technician's manual, in: National Cooperative Highway Research Program Rep. No. 452, 2001.
[29] ASTM International, ASTM D2493. Standard Viscosity–Temperature Chart for Asphalts, American Society for Testing and Materials, Pennsylvania, USA, 2009.
[30] N.I. Yusoff, Modelling the Linear Viscoelastic Rheological Properties of Bituminous Binders PhD Thesis, The University of Nottingham, 2012.

[31] M.L. Williams, R.F. Landel, J.D. Ferry, The temperature dependence of relaxation mechanisms in amorphous polymers and other glass-forming liquids, J. Am. Chem. Soc. 77 (14) (1955) 3701–3707.
[32] N.I.M. Yusoff, F.M. Jakarni, V.H. Nguyen, M.R. Hainin, G.D. Airey, Modelling the rheological properties of bituminous binders using mathematical equations, Constr. Build. Mater. 40 (2013) 174–188.
[33] N.I.M. Yusoff, M.T. Shaw, G.D. Airey, Modelling the linear viscoelastic rheological properties of bituminous binders, Constr. Build. Mater. 25 (5) (2011) 2171–2189.
[34] AASHTO: TP 101, Estimating damage tolerance of asphalt binders using the linear amplitude sweep, in: American Association of State Highway and Transportation Officials Standards for Tests, 2014, pp. 1–7.
[35] R. Micaelo, A. Pereira, L. Quaresma, M.T. Cidade, Fatigue resistance of asphalt binders: assessment of the analysis methods in strain-controlled tests, Constr. Build. Mater. 98 (15) (2015) 703–712.
[36] Belgian Road Research Centre, BRRC ME 85/13: Bitumen Analysis by FTIR Spectrometry: Testing and Analysis Protocol, Belgian Road Research Centre, Brussels, 2013.
[37] H. Kim, H.J. Lee, S. Amirkhanian, Rheology of warm mix asphalt binders with aged binders, Constr. Build. Mater. 25 (2011) 183–189.
[38] B. Colbert, Z. You, The properties of Asphalt Binder blended with variable quantities of recycled asphalt using short term and long term aging simulations, Constr. Build. Mater. 26 (2012) 552–557.
[39] B. Rahimzadeh, Linear and Non-Linear Viscoelastic Behaviour of Binders and Asphalts PhD Thesis, The University of Nottingham, 2002.